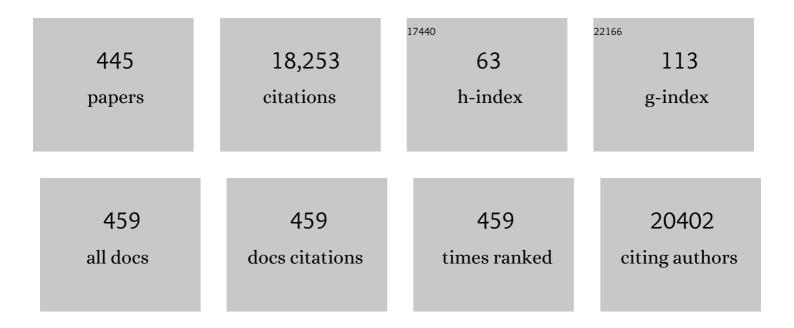
List of Publications by Year in descending order

Source: https://exaly.com/author-pdf/2772110/publications.pdf Version: 2024-02-01



#	Article	IF	CITATIONS
1	Fundamentals of Mesostructuring Through Evaporation-Induced Self-Assembly. Advanced Functional Materials, 2004, 14, 309-322.	14.9	732
2	Fibrillar Structure and Mechanical Properties of Collagen. Journal of Structural Biology, 1998, 122, 119-122.	2.8	539
3	Efficient water oxidation at carbon nanotube–polyoxometalate electrocatalytic interfaces. Nature Chemistry, 2010, 2, 826-831.	13.6	459
4	Structural information from multilamellar liposomes at full hydration: Fullq-range fitting with high quality x-ray data. Physical Review E, 2000, 62, 4000-4009.	2.1	440
5	Effect of polyethyleneglycol (PEG) chain length on the bio–nano-interactions between PEGylated lipid nanoparticles and biological fluids: from nanostructure to uptake in cancer cells. Nanoscale, 2014, 6, 2782.	5.6	433
6	Enhanced Activity of Enzymes Encapsulated in Hydrophilic Metal–Organic Frameworks. Journal of the American Chemical Society, 2019, 141, 2348-2355.	13.7	351
7	Periodically ordered nanoscale islands and mesoporous films composed of nanocrystalline multimetallic oxides. Nature Materials, 2004, 3, 787-792.	27.5	327
8	Highly Porous TiO2 Anatase Optical Thin Films with Cubic Mesostructure Stabilized at 700 °C. Chemistry of Materials, 2003, 15, 4562-4570.	6.7	312
9	First performance assessment of the small-angle X-ray scattering beamline at ELETTRA. Journal of Synchrotron Radiation, 1998, 5, 506-508.	2.4	244
10	Two-Dimensional Hexagonal Mesoporous Silica Thin Films Prepared from Block Copolymers:Â Detailed Characterization and Formation Mechanism. Chemistry of Materials, 2001, 13, 1848-1856.	6.7	233
11	A new method to position and functionalize metal-organic framework crystals. Nature Communications, 2011, 2, 237.	12.8	225
12	Quantification of ion confinement and desolvation in nanoporous carbon supercapacitors with modelling and in situ X-ray scattering. Nature Energy, 2017, 2, .	39.5	210
13	Enzyme Encapsulation in a Porous Hydrogen-Bonded Organic Framework. Journal of the American Chemical Society, 2019, 141, 14298-14305.	13.7	210
14	Platinum nanozymes recover cellular ROS homeostasis in an oxidative stress-mediated disease model. Nanoscale, 2016, 8, 3739-3752.	5.6	203
15	An in Situ Study of Mesostructured CTABâ^'Silica Film Formation during Dip Coating Using Time-Resolved SAXS and Interferometry Measurements. Chemistry of Materials, 2002, 14, 931-939.	6.7	198
16	Humidity-controlled mesostructuration in CTAB-templated silica thin film processing. The existence of a modulable steady state. Journal of Materials Chemistry, 2003, 13, 61-66.	6.7	193
17	Degradation of ZIF-8 in phosphate buffered saline media. CrystEngComm, 2019, 21, 4538-4544.	2.6	186
18	Thermally Stable Nanocrystalline γ-Alumina Layers with Highly Ordered 3D Mesoporosity. Angewandte Chemie - International Edition, 2005, 44, 4589-4592.	13.8	182

#	Article	IF	CITATIONS
19	Growth Kinetics of ZnO Nanocrystals:Â A Few Surprises. Journal of the American Chemical Society, 2007, 129, 4470-4475.	13.7	166
20	Interplay of protein corona and immune cells controls blood residency of liposomes. Nature Communications, 2019, 10, 3686.	12.8	160
21	Characteristics of mineral particles in the human bone/cartilage interface. Journal of Structural Biology, 2003, 141, 208-217.	2.8	153
22	Perovskite-type superlattices from lead halide perovskite nanocubes. Nature, 2021, 593, 535-542.	27.8	152
23	In Situ Synchrotron Small-Angle X-ray Scattering/X-ray Diffraction Study of the Formation of SBA-15 Mesoporous Silica. Langmuir, 2004, 20, 4885-4891.	3.5	150
24	Enhanced Cutinase-Catalyzed Hydrolysis of Polyethylene Terephthalate by Covalent Fusion to Hydrophobins. Applied and Environmental Microbiology, 2015, 81, 3586-3592.	3.1	149
25	Stable Ultraconcentrated and Ultradilute Colloids of CsPbX ₃ (X = Cl, Br) Nanocrystals Using Natural Lecithin as a Capping Ligand. Journal of the American Chemical Society, 2019, 141, 19839-19849.	13.7	141
26	Self-assembly of large, ordered lamellae from non-bilayer lipids and integral membrane proteins in vitro. Proceedings of the National Academy of Sciences of the United States of America, 2000, 97, 1473-1476.	7.1	138
27	Differential Modulation of Membrane Structure and Fluctuations by Plant Sterols and Cholesterol. Biophysical Journal, 2008, 94, 3935-3944.	0.5	136
28	Highâ€flux beamline for smallâ€angle xâ€ray scattering at ELETTRA. Review of Scientific Instruments, 1995, 66, 1624-1626.	1.3	134
29	SAXS Study of the Nucleation of Glycine Crystals from a Supersaturated Solution. Crystal Growth and Design, 2005, 5, 523-527.	3.0	133
30	Highly Luminescent Metal–Organic Frameworks Through Quantum Dot Doping. Small, 2012, 8, 80-88.	10.0	132
31	Hierarchical organization of perylene bisimides and polyoxometalates for photo-assisted water oxidation. Nature Chemistry, 2019, 11, 146-153.	13.6	132
32	Kinetics of Cosurfactantâ^'Surfactantâ^'Silicate Phase Behavior. 1. Short-Chain Alcohols. Journal of Physical Chemistry B, 1999, 103, 5943-5948.	2.6	128
33	Tracking the structural arrangement of ions in carbon supercapacitor nanopores using in situ small-angle X-ray scattering. Energy and Environmental Science, 2015, 8, 1725-1735.	30.8	126
34	Performance and First Results of the ELETTRA High-Flux Beamline for Small-Angle X-ray Scattering. Journal of Applied Crystallography, 1997, 30, 872-876.	4.5	124
35	Nanocrystalline Mesoporous γ-Alumina Powders "UPMC1 Material―Gathers Thermal and Chemical Stability with High Surface Area. Chemistry of Materials, 2006, 18, 5238-5243.	6.7	118
36	Silica Orthorhombic Mesostructured Films with Low Refractive Index and High Thermal Stability. Journal of Physical Chemistry B, 2004, 108, 10942-10948.	2.6	114

#	Article	IF	CITATIONS
37	Discovery of New Hexagonal Supramolecular Nanostructures Formed by Squalenoylation of an Anticancer Nucleoside Analogue. Small, 2008, 4, 247-253.	10.0	114
38	Direct X-ray and electron-beam lithography of halogenated zeolitic imidazolate frameworks. Nature Materials, 2021, 20, 93-99.	27.5	112
39	Investigation of Cu ₂ ZnSnS ₄ Formation from Metal Salts and Thioacetamide. Chemistry of Materials, 2010, 22, 3399-3406.	6.7	109
40	Transfection efficiency boost of cholesterol-containing lipoplexes. Biochimica Et Biophysica Acta - Biomembranes, 2012, 1818, 2335-2343.	2.6	102
41	Monodisperse Iron Oxide Nanoparticles by Thermal Decomposition: Elucidating Particle Formation by Second-Resolved in Situ Small-Angle X-ray Scattering. Chemistry of Materials, 2017, 29, 4511-4522.	6.7	102
42	Evolution of the Protein Corona of Lipid Gene Vectors as a Function of Plasma Concentration. Langmuir, 2011, 27, 15048-15053.	3.5	101
43	Interaction of LL-37 with Model Membrane Systems of Different Complexity: Influence of the Lipid Matrix. Biophysical Journal, 2008, 94, 4688-4699.	0.5	96
44	Encapsulation, Visualization and Expression of Genes with Biomimetically Mineralized Zeolitic Imidazolate Frameworkâ€8 (ZIFâ€8). Small, 2019, 15, e1902268.	10.0	95
45	Cationic liposome/DNA complexes: from structure to interactions with cellular membranes. European Biophysics Journal, 2012, 41, 815-829.	2.2	93
46	Formation of Interpenetrating Hierarchical Titania Structures by Confined Synthesis in Inverse Opal. Journal of the American Chemical Society, 2011, 133, 17274-17282.	13.7	90
47	Impurities in Commercial Phytantriol Significantly Alter Its Lyotropic Liquid-Crystalline Phase Behavior. Langmuir, 2008, 24, 6998-7003.	3.5	89
48	Combining structure and dynamics: non-denaturing high-pressure effect on lysozyme in solution. Journal of the Royal Society Interface, 2009, 6, S619-34.	3.4	86
49	Snapshots into carbon dots formation through a combined spectroscopic approach. Nature Communications, 2021, 12, 2640.	12.8	86
50	Influence of the degree of scandium supersaturation on the precipitation kinetics of rapidly solidified Al-Mg-Sc-Zr alloys. Acta Materialia, 2016, 117, 43-50.	7.9	85
51	Salt concentration and charging velocity determine ion charge storage mechanism in nanoporous supercapacitors. Nature Communications, 2018, 9, 4145.	12.8	85
52	Investigation of the Formation of CuInS ₂ Nanoparticles by the Oleylamine Route: Comparison of Microwave-Assisted and Conventional Syntheses. Inorganic Chemistry, 2011, 50, 193-200.	4.0	84
53	Structural Characterization of Siliceous Spicules from Marine Sponges. Biophysical Journal, 2004, 86, 526-534.	0.5	79
54	Order vs. disorder—a huge increase in ionic conductivity of nanocrystalline LiAlO2 embedded in an amorphous-like matrix of lithium aluminate. Journal of Materials Chemistry A, 2014, 2, 20295-20306.	10.3	79

#	Article	IF	CITATIONS
55	Lipid composition: a "key factor―for the rational manipulation of the liposome–protein corona by liposome design. RSC Advances, 2015, 5, 5967-5975.	3.6	77
56	A structurally diverse library of safe-by-design citrem-phospholipid lamellar and non-lamellar liquid crystalline nano-assemblies. Journal of Controlled Release, 2016, 239, 1-9.	9.9	76
57	Nanostructured Polymers Obtained from Polyethylene-block-poly(ethylene oxide) Block Copolymer in Unsaturated Polyester. Macromolecules, 2007, 40, 2532-2538.	4.8	75
58	Monodisperse Long-Chain Sulfobetaine-Capped CsPbBr ₃ Nanocrystals and Their Superfluorescent Assemblies. ACS Central Science, 2021, 7, 135-144.	11.3	75
59	In Situ Determination of Structure and Fluctuations of Coexisting Fluid Membrane Domains. Biophysical Journal, 2015, 108, 854-862.	0.5	73
60	Self-Assembly and Crystallization Behavior of Mesoporous, Crystalline HfO2 Thin Films: A Model System for the Generation of Mesostructured Transition-Metal Oxides. Small, 2005, 1, 889-898.	10.0	72
61	Time-Resolved in Situ Studies of the Formation of Cubic Mesoporous Silica Formed with Triblock Copolymers. Langmuir, 2004, 20, 10311-10316.	3.5	70
62	Highly Ordered "Defect-Free―Self-Assembled Hybrid Films with a Tetragonal Mesostructure. Journal of the American Chemical Society, 2005, 127, 3838-3846.	13.7	69
63	A Chemical Solution Deposition Route To Nanopatterned Inorganic Material Surfaces. Chemistry of Materials, 2007, 19, 3717-3725.	6.7	67
64	Multicomponent Cationic Lipidâ `DNA Complex Formation:Â Role of Lipid Mixing. Langmuir, 2005, 21, 11582-11587.	3.5	65
65	Differential regulation of human papillomavirus E6 by protein kinase A: conditional degradation of human discs large protein by oncogenic E6. Oncogene, 2000, 19, 5884-5891.	5.9	64
66	First in-situ SAXS studies of the mesostructuration of spherical silica and titania particles during spray-drying process. Chemical Communications, 2003, , 2798-2799.	4.1	64
67	Dynamic Control of MOFâ€5 Crystal Positioning Using a Magnetic Field. Advanced Materials, 2011, 23, 3901-3906.	21.0	64
68	Fabrication of Advanced Functional Devices Combining Soft Chemistry with Xâ€ray Lithography in One Step. Advanced Materials, 2009, 21, 4932-4936.	21.0	63
69	Two-Dimensional-Hexagonal Periodic Mesoporous Polymer Resin Thin Films by Soft Templating. Chemistry of Materials, 2009, 21, 5754-5762.	6.7	62
70	Global small-angle X-ray scattering data analysis for multilamellar vesicles: the evolution of the scattering density profile model. Journal of Applied Crystallography, 2014, 47, 173-180.	4.5	62
71	New evidence for gel-liquid crystalline phase coexistence in the ripple phase of phosphatidylcholines. European Biophysics Journal, 2000, 29, 125-133.	2.2	61
72	Title is missing!. Journal of Sol-Gel Science and Technology, 2003, 26, 561-565.	2.4	61

#	Article	IF	CITATIONS
73	Structural, dynamic and mechanical properties of POPC at low cholesterol concentration studied in pressure/temperature space. European Biophysics Journal, 2003, 31, 575-585.	2.2	61
74	Nonequilibrium Effects in Self-Assembled Mesophase Materials: Unexpected Supercooling Effects for Cubosomes and Hexosomes. Langmuir, 2010, 26, 9000-9010.	3.5	61
75	The new high resolution ultra small-angle neutron scattering instrument at the High Flux Reactor in Grenoble. Journal of Applied Crystallography, 2000, 33, 851-854.	4.5	59
76	Structure and fluctuations of phosphatidylcholines in the vicinity of the main phase transition. Physical Review E, 2004, 70, 021908.	2.1	58
77	Observation of Local Order in Poly(di-n-alkyl itaconate)s. Macromolecules, 2000, 33, 4989-4991.	4.8	57
78	Hierarchical Porous Silica Films with Ultralow Refractive Index. Chemistry of Materials, 2009, 21, 2055-2061.	6.7	57
79	Transfection efficiency boost by designer multicomponent lipoplexes. Biochimica Et Biophysica Acta - Biomembranes, 2007, 1768, 2280-2292.	2.6	56
80	Free jet micromixer to study fast chemical reactions by small angle X-ray scattering. Lab on A Chip, 2009, 9, 2063.	6.0	56
81	Relationship between Self-Association of Glycine Molecules in Supersaturated Solutions and Solid State Outcome. Physical Review Letters, 2007, 99, 115702.	7.8	55
82	In Situ SAXS Study on a New Mechanism for Mesostructure Formation of Ordered Mesoporous Carbons: Thermally Induced Self-Assembly. Journal of the American Chemical Society, 2012, 134, 11136-11145.	13.7	55
83	Continuousâ€Flow Synthesis of ZIFâ€8 Biocomposites with Tunable Particle Size. Angewandte Chemie - International Edition, 2020, 59, 8123-8127.	13.8	55
84	Scanning X-ray diffraction peak profile analysis in deformed Cu-polycrystals by synchrotron radiation1This work is dedicated to Professor Dr Guenther Schoeck on the occasion of his 70th birthday.1. Acta Materialia, 1999, 47, 1053-1061.	7.9	54
85	Salt-induced phase separation in the liquid crystalline phase of phosphatidylcholines. Colloids and Surfaces A: Physicochemical and Engineering Aspects, 2001, 183-185, 171-181.	4.7	54
86	Time-Resolved Simultaneous Detection of Structural and Chemical Changes during Self-Assembly of Mesostructured Films. Journal of Physical Chemistry C, 2007, 111, 5345-5350.	3.1	54
87	Structural Investigation of Bulk and Dispersed Inverse Lyotropic Hexagonal Liquid Crystalline Phases of Eicosapentaenoic Acid Monoglyceride. Langmuir, 2017, 33, 14045-14057.	3.5	54
88	Hexagonally organised mesoporous aluminium–oxo–hydroxide thin films prepared by the template approach. In situ study of the structural formation. Journal of Materials Chemistry, 2002, 12, 557-564.	6.7	53
89	PbS-Doped Mesostructured Silica Films with High Optical Nonlinearity. Chemistry of Materials, 2005, 17, 4965-4970.	6.7	52
90	Effects of Pressure and Temperature on the Self-Assembled Fully Hydrated Nanostructures of Monooleinâ ´'Oil Systems. Langmuir, 2010, 26, 1177-1185.	3.5	52

#	Article	IF	CITATIONS
91	Core–Shell Structure of Monodisperse Poly(ethylene glycol)-Grafted Iron Oxide Nanoparticles Studied by Small-Angle X-ray Scattering. Chemistry of Materials, 2015, 27, 4763-4771.	6.7	52
92	Factors Determining the Superior Performance of Lipid/DNA/Protammine Nanoparticles over Lipoplexes. Journal of Medicinal Chemistry, 2011, 54, 4160-4171.	6.4	51
93	Top-down patterning of Zeolitic Imidazolate Framework composite thin films by deep X-ray lithography. Chemical Communications, 2012, 48, 7483.	4.1	51
94	Human Biomolecular Corona of Liposomal Doxorubicin: The Overlooked Factor in Anticancer Drug Delivery. ACS Applied Materials & Interfaces, 2018, 10, 22951-22962.	8.0	51
95	Surfactant-Mediated Generation of Iso-Oriented Dense and Mesoporous Crystalline Metal-Oxide Layers. Advanced Materials, 2006, 18, 1827-1831.	21.0	50
96	Structural and Functional Insights into the DNA Replication Factor Cdc45 Reveal an Evolutionary Relationship to the DHH Family of Phosphoesterases. Journal of Biological Chemistry, 2012, 287, 4121-4128.	3.4	49
97	Phase transformation during cubic mesostructured silica film formation. Chemical Communications, 2002, , 748-749.	4.1	48
98	Mesostructured self-assembled titania films for photovoltaic applications. Microporous and Mesoporous Materials, 2006, 88, 304-311.	4.4	48
99	Solvent Molding of Organic Morphologies Made of Supramolecular Chiral Polymers. Journal of the American Chemical Society, 2015, 137, 8150-8160.	13.7	48
100	Influence of antimicrobial peptides on the formation of nonlamellar lipid mesophases. Biochimica Et Biophysica Acta - Biomembranes, 2008, 1778, 2325-2333.	2.6	47
101	Toward the Rational Design of Lipid Gene Vectors: Shape Coupling between Lipoplex and Anionic Cellular Lipids Controls the Phase Evolution of Lipoplexes and the Efficiency of DNA Release. ACS Applied Materials & Interfaces, 2009, 1, 2237-2249.	8.0	47
102	Carbohydrates@MOFs. Materials Horizons, 2019, 6, 969-977.	12.2	46
103	High-Throughput Asymmetric Double-Crystal Monochromator of the SAXS Beamline at ELETTRA. Journal of Synchrotron Radiation, 1998, 5, 1215-1221.	2.4	45
104	Structural Stability against Disintegration by Anionic Lipids Rationalizes the Efficiency of Cationic Liposome/DNA Complexes. Langmuir, 2007, 23, 4498-4508.	3.5	45
105	Fabrication of Mesoporous Functionalized Arrays by Integrating Deep Xâ€Ray Lithography with Dipâ€Pen Writing. Advanced Materials, 2008, 20, 1864-1869.	21.0	45
106	Nanocomposite mesoporous ordered films for lab-on-chip intrinsic surface enhanced Raman scattering detection. Nanoscale, 2011, 3, 3760.	5.6	45
107	CuInS2–Poly(3-(ethyl-4-butanoate)thiophene) nanocomposite solar cells: Preparation by an in situ formation route, performance and stability issues. Solar Energy Materials and Solar Cells, 2011, 95, 1354-1361.	6.2	45
108	Cross-Linked Carbon Nanotube Adsorbents for Water Treatment: Tuning the Sorption Capacity through Chemical Functionalization. ACS Applied Materials & Interfaces, 2019, 11, 12920-12930.	8.0	45

#	Article	IF	CITATIONS
109	Polymer/Nanocrystal Hybrid Solar Cells: Influence of Molecular Precursor Design on Film Nanomorphology, Charge Generation and Device Performance. Advanced Functional Materials, 2015, 25, 409-420.	14.9	44
110	Modulation of metal-azolate frameworks for the tunable release of encapsulated glycosaminoglycans. Chemical Science, 2020, 11, 10835-10843.	7.4	44
111	Tailoring Lipoplex Composition to the Lipid Composition of Plasma Membrane: A Trojan Horse for Cell Entry?. Langmuir, 2010, 26, 13867-13873.	3.5	43
112	Position Accuracy of Gold Nanoparticles on DNA Origami Structures Studied with Small-Angle X-ray Scattering. Nano Letters, 2018, 18, 2609-2615.	9.1	43
113	High-pressure instrument for small- and wide-angle x-ray scattering. II. Time-resolved experiments. Review of Scientific Instruments, 1999, 70, 1540-1545.	1.3	42
114	Solubilization of Oil in Silicateâ^'Surfactant Mesostructures. Langmuir, 2000, 16, 5831-5836.	3.5	42
115	Non-equilibrium formation of the cubic Pn 3 m phase in a monoolein/water system. Europhysics Letters, 2006, 75, 267-273.	2.0	42
116	Bottom-up Approach toward Titanosilicate Mesoporous Pillared Planar Nanochannels for Nanofluidic Applications. Chemistry of Materials, 2010, 22, 5687-5694.	6.7	42
117	Formation and Stabilization of Mesostructured Vanadium-Oxo-Based Hybrid Thin Films. Chemistry of Materials, 2002, 14, 3316-3325.	6.7	41
118	Controlled Solubilization of Toluene by Silicateâ	3.5	41
119	Fat Crystallization in Emulsion:  Influence of Emulsifier Concentration on Triacylglycerol Crystal Growth and Polymorphism. Crystal Growth and Design, 2004, 4, 1283-1293.	3.0	41
120	Enhanced Transfection Efficiency of Multicomponent Lipoplexes in the Regime of Optimal Membrane Charge Density. Journal of Physical Chemistry B, 2008, 112, 11298-11304.	2.6	41
121	Structural Stability and Increase in Size Rationalize the Efficiency of Lipoplexes in Serum. Langmuir, 2009, 25, 3013-3021.	3.5	41
122	Small Angle X-ray Scattering Analysis of Deoxyguanosine 5′-Monophosphate Self-Assembing in Solution: Nucleation and Growth of G-Quadruplexes. Journal of Physical Chemistry B, 2009, 113, 7934-7944.	2.6	41
123	Existence of hybrid structures in cationic liposome/DNA complexes revealed by their interaction with plasma proteins. Colloids and Surfaces B: Biointerfaces, 2011, 82, 141-146.	5.0	41
124	Magnetically responsive horseradish peroxidase@ZIF-8 for biocatalysis. Chemical Communications, 2020, 56, 5775-5778.	4.1	41
125	Nanocasted mesoporous nanocrystalline ZnO thin films. Journal of Materials Chemistry, 2010, 20, 537-542.	6.7	40
126	A carbon nanopore model to quantify structure and kinetics of ion electrosorption with in situ small-angle X-ray scattering. Physical Chemistry Chemical Physics, 2017, 19, 15549-15561.	2.8	39

#	Article	IF	CITATIONS
127	In situ Synchrotron SAXS/XRD Study on the Formation of Ordered Mesoscopic Hybrid Materials with Crystal-Like Walls. Chemistry of Materials, 2004, 16, 5564-5566.	6.7	38
128	The effect of graphene on liquid-crystalline blue phases. Applied Physics Letters, 2013, 103, .	3.3	38
129	Surface-Sensitive Approach to Interpreting Supramolecular Rearrangements in Cellulose by Synchrotron Grazing Incidence Small-Angle X-ray Scattering. ACS Macro Letters, 2015, 4, 713-716.	4.8	38
130	Investigation of bone and cartilage by synchrotron scanning-SAXS and -WAXD with micrometer spatial resolution. Journal of Applied Crystallography, 2000, 33, 820-823.	4.5	37
131	Kinetics of Cosurfactantâ^'Surfactantâ^'Silicate Phase Behavior. 2. Short-Chain Aminesâ€. Langmuir, 2000, 16, 8809-8813.	3.5	37
132	Direct nano-in-micropatterning of TiO2 thin layers and TiO2/Pt nanoelectrode arrays by deep X-ray lithography. Journal of Materials Chemistry, 2011, 21, 3597.	6.7	36
133	The Role Played by Salts in the Formation of SBA-15, an in Situ Small-Angle X-ray Scattering/Diffraction Study. Langmuir, 2011, 27, 7121-7131.	3.5	36
134	Effects of resveratrol on the structure and fluidity of lipid bilayers: a membrane biophysical study. Soft Matter, 2016, 12, 2118-2126.	2.7	36
135	<i>In situ</i> tensile testing of human aortas by time-resolved small-angle X-ray scattering. Journal of Synchrotron Radiation, 2005, 12, 727-733.	2.4	35
136	Thermal-induced phase transitions in self-assembled mesostructured films studied by small-angle X-ray scattering. Journal of Synchrotron Radiation, 2005, 12, 734-738.	2.4	35
137	Depth profiling of marker layers using x-ray waveguide structures. Physical Review B, 2005, 72, .	3.2	35
138	The critical role of water in spider silk and its consequence for protein mechanics. Nanoscale, 2011, 3, 3805.	5.6	35
139	Stabilization of supramolecular membrane protein–lipid bilayer assemblies through immobilization in a crystalline exoskeleton. Nature Communications, 2021, 12, 2202.	12.8	35
140	Synthesis, characterization and optical properties of Eu2O3mesoporous thin films. Nanotechnology, 2007, 18, 055705.	2.6	34
141	Writing Self-Assembled Mesostructured Films with In situ Formation of Gold Nanoparticles. Chemistry of Materials, 2010, 22, 2132-2137.	6.7	34
142	Monitoring fat crystallization in aerated food emulsions by combined DSC and time-resolved synchrotron X-ray diffraction. Food Research International, 2002, 35, 927-934.	6.2	33
143	Lipid mixing upon deoxyribonucleic acid-induced liposomes fusion investigated by synchrotron small-angle x-ray scattering. Applied Physics Letters, 2005, 87, 133901.	3.3	33
144	Interaction of a new anticancer prodrug, gemcitabine–squalene, with a model membrane. Biochimica Et Biophysica Acta - Biomembranes, 2010, 1798, 1522-1532.	2.6	33

#	Article	IF	CITATIONS
145	Transfer of lipid and phase reorganisation in self-assembled liquid crystal nanostructured particles based on phytantriol. Physical Chemistry Chemical Physics, 2011, 13, 3026.	2.8	33
146	Interaction of Lipoplexes with Anionic Lipids Resulting in DNA Release is a Two-Stage Process. Langmuir, 2007, 23, 8713-8717.	3.5	32
147	X-ray Kinematography of Temperature-Jump Relaxation Probes the Elastic Properties of Fluid Bilayersâ€. Langmuir, 2000, 16, 8994-9001.	3.5	31
148	Presmectic wetting and supercritical-like phase behavior of octylcyanobiphenyl liquid crystal confined to controlled-pore glass matrices. Journal of Chemical Physics, 2007, 127, 154905.	3.0	31
149	In Situ Monitoring of Nanostructure Formation during the Digestion of Mayonnaise. ACS Omega, 2017, 2, 1441-1446.	3.5	31
150	Chemical Stability of Mesoporous Oxide Thin Film Electrodes under Electrochemical Cycling: from Dissolution to Stabilization. Langmuir, 2019, 35, 6279-6287.	3.5	31
151	Phospholipid mesophases at solid interfaces: in-situ X-ray diffraction and spin-label studies. Advances in Colloid and Interface Science, 2004, 111, 63-77.	14.7	30
152	Highly ordered self-assembled mesostructured membranes: Porous structure and pore surface coverage. Microporous and Mesoporous Materials, 2007, 103, 113-122.	4.4	30
153	Hierarchical Formation Mechanism of CoFe ₂ O ₄ Mesoporous Assemblies. ACS Nano, 2015, 9, 7277-7286.	14.6	30
154	Killing cancer cells using nanotechnology: novel poly(I:C) loaded liposome–silica hybrid nanoparticles. Journal of Materials Chemistry B, 2015, 3, 7408-7416.	5.8	30
155	Conversion of Copper Carbonate into a Metal–Organic Framework. Chemistry of Materials, 2018, 30, 5630-5638.	6.7	30
156	Ordered Mesoporous Silicate Structures as Potential Templates for Nanowire Growth. Advanced Functional Materials, 2007, 17, 133-141.	14.9	29
157	Control and Analysis of Oriented Thin Films of Lipid Inverse Bicontinuous Cubic Phases Using Grazing Incidence Small-Angle X-ray Scattering. Langmuir, 2013, 29, 9874-9880.	3.5	29
158	In Situ Measurement of Electrosorption-Induced Deformation Reveals the Importance of Micropores in Hierarchical Carbons. ACS Applied Materials & amp; Interfaces, 2017, 9, 23319-23324.	8.0	29
159	In-situ aerosol nanoparticle characterization by small angle X-ray scattering at ultra-low volume fraction. Nature Communications, 2019, 10, 1122.	12.8	29
160	How lipid hydration and temperature affect the structure of DC-Chol–DOPE/DNA lipoplexes. Chemical Physics Letters, 2006, 422, 439-445.	2.6	28
161	Confined growth of iron cobalt nanocrystals in mesoporous silica thin films: FeCo–SiO2 nanocomposites. Microporous and Mesoporous Materials, 2008, 115, 338-344.	4.4	28
162	Surface Passivation Improves the Synthesis of Highly Stable and Specific DNA-Functionalized Gold Nanoparticles with Variable DNA Density. ACS Applied Materials & Interfaces, 2015, 7, 7033-7040.	8.0	28

#	Article	IF	CITATIONS
163	Opsonin-Deficient Nucleoproteic Corona Endows UnPEGylated Liposomes with Stealth Properties <i>In Vivo</i> . ACS Nano, 2022, 16, 2088-2100.	14.6	28
164	Time-resolved SAXS study of crystallization of poly(ethylene oxide)/poly(methyl methacrylate) blends. Polymer, 1999, 40, 439-445.	3.8	27
165	Fiber diffraction study of spicules from marine sponges. Microscopy Research and Technique, 2003, 62, 378-381.	2.2	27
166	Exfoliated Graphene into Highly Ordered Mesoporous Titania Films: Highly Performing Nanocomposites from Integrated Processing. ACS Applied Materials & Interfaces, 2014, 6, 795-802.	8.0	27
167	In vitro and in vivo performance of monoacyl phospholipid-based self-emulsifying drug delivery systems. Journal of Controlled Release, 2017, 255, 45-53.	9.9	27
168	Preparation of multi-nanocrystalline transition metal oxide (TiO2–NiTiO3) mesoporous thin films. New Journal of Chemistry, 2005, 29, 141-144.	2.8	26
169	Detailed study of the pore-filling processes during nanocasting of mesoporous films using SnO2/SiO2 as a model system. Microporous and Mesoporous Materials, 2009, 123, 185-192.	4.4	26
170	Implication of Sphingomyelin/Ceramide Molar Ratio on the Biological Activity of Sphingomyelinase. Biophysical Journal, 2010, 99, 499-506.	0.5	26
171	Densification of sol–gel silica thin films induced by hard X-rays generated by synchrotron radiation. Journal of Synchrotron Radiation, 2011, 18, 280-286.	2.4	26
172	Exploring the interactions of irbesartan and irbesartan–2-hydroxypropyl-β-cyclodextrin complex with model membranes. Biochimica Et Biophysica Acta - Biomembranes, 2017, 1859, 1089-1098.	2.6	26
173	Aggregation-Induced Energy Transfer in a Decanuclear Os(II)/Ru(II) Polypyridine Light-Harvesting Antenna Dendrimer. CheM, 2017, 3, 494-508.	11.7	26
174	Small-angle X-ray scattering from micellar solutions of gemini surfactants. Chemical Physics Letters, 2000, 329, 336-340.	2.6	25
175	Bile salts form lyotropic liquid crystals. Colloids and Surfaces A: Physicochemical and Engineering Aspects, 2003, 213, 79-92.	4.7	25
176	Effect of the Electrostatic Charge on the Mechanism Inducing Liposome Solubilization:Â A Kinetic Study by Synchrotron Radiation SAXS. Langmuir, 2004, 20, 3074-3079.	3.5	25
177	Highly Ordered Self-Assembled Mesostructured Hafnia Thin Films:Â An Example of Rewritable Mesostructure. Chemistry of Materials, 2006, 18, 4553-4560.	6.7	25
178	Structural Transitions in Asymmetric Poly(styrene)- <i>block</i> -Poly(lactide) Thin Films Induced by Solvent Vapor Exposure. ACS Applied Materials & Interfaces, 2014, 6, 12146-12152.	8.0	25
179	Manipulation of lipoplex concentration at the cell surface boosts transfection efficiency in hard-to-transfect cells. Nanomedicine: Nanotechnology, Biology, and Medicine, 2017, 13, 681-691.	3.3	25
180	Microfluidic Formulation of DNA-Loaded Multicomponent Lipid Nanoparticles for Gene Delivery. Pharmaceutics, 2021, 13, 1292.	4.5	25

#	Article	IF	CITATIONS
181	Collagen fibrils are differently organized in weight-bearing and not-weight-bearing regions of pig articular cartilage. The Journal of Experimental Zoology, 2000, 287, 346-352.	1.4	24
182	Changes in myosin S1 orientation and force induced by a temperature increase. Proceedings of the National Academy of Sciences of the United States of America, 2002, 99, 5384-5389.	7.1	24
183	In-Situ SAXS Studies on the Formation of Silicate/Surfactant Mesophases with Solubilized Benzene under Acidic Conditions. Langmuir, 2002, 18, 10053-10057.	3.5	24
184	One-pot self-assembly of mesostructured silica films and membranes functionalised with fullerene derivativesElectronic supplementary information (ESI) available: selected analytical data of 2 and 3. See http://www.rsc.org/suppdata/jm/b4/b401916d/. Journal of Materials Chemistry, 2004, 14, 1838.	6.7	24
185	Electrical responses of silica mesostructured films to changes in environmental humidity and processing conditions. Journal of Non-Crystalline Solids, 2005, 351, 1980-1986.	3.1	24
186	Role of temperature-independent lipoplex–cell membrane interactions in the efficiency boost of multicomponent lipoplexes. Cancer Gene Therapy, 2011, 18, 543-552.	4.6	24
187	Lipid Sorting by Ceramide and the Consequences for Membrane Proteins. Biophysical Journal, 2012, 102, 2031-2038.	0.5	24
188	Dimensional crossover and scaling behavior of a smectic liquid crystal confined to controlled-pore glass matrices. Soft Matter, 2012, 8, 2460.	2.7	24
189	Growth of fractal aggregates during template directed SAPO-34 zeolite formation. Microporous and Mesoporous Materials, 2013, 167, 3-9.	4.4	24
190	Biobased Cellulosic–CuInS ₂ Nanocomposites for Optoelectronic Applications. ACS Sustainable Chemistry and Engineering, 2017, 5, 3115-3122.	6.7	24
191	Impact of the biomolecular corona on the structure of PEGylated liposomes. Biomaterials Science, 2017, 5, 1884-1888.	5.4	24
192	Phase-separation kinetics of a multicomponent alloy. Physical Review B, 1999, 60, 822-830.	3.2	23
193	Ordered Mesostructured Silica Films: Effect of Pore Surface on its Sensing Properties. Journal of Sol-Gel Science and Technology, 2004, 32, 107-110.	2.4	23
194	One-Dimensional Thermotropic Dilatation Area of Lipid Headgroups within Lamellar Lipid/DNA Complexes. Langmuir, 2006, 22, 4267-4273.	3.5	23
195	Shaping Mesoporous Films Using Dewetting on X-ray Pre-patterned Hydrophilic/Hydrophobic Layers and Pinning Effects at the Pattern Edge. Langmuir, 2011, 27, 3898-3905.	3.5	23
196	Substrate and drying effect in shape and ordering of micelles inside CTAB–silica mesostructured films. Soft Matter, 2012, 8, 2956.	2.7	23
197	Self-Assembly in Poly(dimethylsiloxane)–Poly(ethylene oxide) Block Copolymer Template Directed Synthesis of Linde Type A Zeolite. Langmuir, 2013, 29, 7079-7086.	3.5	23
198	Direct monitoring of lipid transfer on exposure of citrem nanoparticles to an ethanol solution containing soybean phospholipids by combining synchrotron SAXS with microfluidics. Analyst, The, 2017, 142, 3118-3126.	3.5	23

#	Article	IF	CITATIONS
199	Selfâ€Assembly of Oriented Antibodyâ€Decorated Metal–Organic Framework Nanocrystals for Activeâ€Targeting Applications. Advanced Materials, 2022, 34, e2106607.	21.0	23
200	Design of transition metal oxide mesoporous thin films. Studies in Surface Science and Catalysis, 2002, 141, 235-242.	1.5	22
201	SAXS investigation on aggregation phenomena in supercritical CO2. European Physical Journal E, 2002, 8, 311-314.	1.6	22
202	Monitoring early stages of silver particle formation in a polymer solution by in situ and time resolved small angle X-ray scattering. Nanoscale, 2010, 2, 2447.	5.6	22
203	Universality of DNA Adsorption Behavior on the Cationic Membranes of Nanolipoplexes. Journal of Physical Chemistry B, 2010, 114, 2028-2032.	2.6	22
204	Accessing Ultrashort Reaction Times in Particle Formation with SAXS Experiments: ZnS Precipitation on the Microsecond Time Scale. Journal of the American Chemical Society, 2010, 132, 6822-6826.	13.7	22
205	Chemical Tailoring of Hybrid Solâ ´`Gel Thick Coatings As Hosting Matrix for Functional Patterned Microstructures. ACS Applied Materials & Interfaces, 2011, 3, 245-251.	8.0	22
206	Combining Top-Down and Bottom-Up Routes for Fabrication of Mesoporous Titania Films Containing Ceria Nanoparticles for Free Radical Scavenging. ACS Applied Materials & Interfaces, 2013, 5, 3168-3175.	8.0	22
207	Enhanced Photocatalytic Activity in Low-Temperature Processed Titania Mesoporous Films. Journal of Physical Chemistry C, 2014, 118, 12000-12009.	3.1	22
208	Tracking morphologies at the nanoscale: Self-assembly of an amphiphilic designer peptide into a double helix superstructure. Nano Research, 2015, 8, 1822-1833.	10.4	22
209	Peptide self-assembly into lamellar phases and the formation of lipid-peptide nanostructures. Nano Research, 2018, 11, 913-928.	10.4	22
210	Evolution of the PtNi Bimetallic Alloy Fuel Cell Catalyst under Simulated Operational Conditions. ACS Applied Materials & Interfaces, 2020, 12, 17602-17610.	8.0	22
211	Low Density Lipoproteins as Circulating Fast Temperature Sensors. PLoS ONE, 2008, 3, e4079.	2.5	22
212	Niobia-stabilised anatase TiO2 highly porous mesostructured thin films. Microporous and Mesoporous Materials, 2006, 94, 208-213.	4.4	21
213	Mesoporous Aluminophosphate Thin Films with Cubic Pore Arrangement. Langmuir, 2008, 24, 6220-6225.	3.5	21
214	Periodic Mesoporous Organosilica in Confined Environments. Chemistry - A European Journal, 2009, 15, 6645-6650.	3.3	21
215	Self-Assembly of Shape Controlled Hierarchical Porous Thin Films: Mesopores and Nanoboxes. Chemistry of Materials, 2009, 21, 4846-4850.	6.7	21
216	Humidity-driven deformation of ordered mesoporous silica films. Bioinspired, Biomimetic and Nanobiomaterials, 2014, 3, 183-190.	0.9	21

#	Article	IF	CITATIONS
217	Peering into the Mechanism of Low-Temperature Synthesis of Bronze-type TiO ₂ in Ionic Liquids. Crystal Growth and Design, 2017, 17, 5586-5601.	3.0	21
218	Structural insights into pH-responsive drug release of self-assembling human serum albumin-silk fibroin nanocapsules. European Journal of Pharmaceutics and Biopharmaceutics, 2018, 133, 176-187.	4.3	21
219	Continuousâ€Flow Synthesis of ZIFâ€8 Biocomposites with Tunable Particle Size. Angewandte Chemie, 2020, 132, 8200-8204.	2.0	21
220	Detailed in Situ XRD and Calorimetric Study of the Formation of Silicate/Mixed Surfactant Mesophases under Alkaline Conditions. Influence of Surfactant Chain Length and Synthesis Temperature. Journal of Physical Chemistry B, 2006, 110, 16254-16260.	2.6	20
221	Effect of hydration on the structure of solid-supported Niosomal membranes investigated by in situ energy dispersive X-ray diffraction. Chemical Physics Letters, 2008, 462, 307-312.	2.6	20
222	One-Step Synthesis of Mesoporous Silica Thin Films Containing Available COOH Groups. ACS Omega, 2017, 2, 4548-4555.	3.5	20
223	Templateâ€Mediated Control over Polymorphism in the Vaporâ€Assisted Formation of Zeolitic Imidazolate Framework Powders and Films. Angewandte Chemie - International Edition, 2021, 60, 7553-7558.	13.8	20
224	SAXS study of the influence of ethanol on the microstructure of polyurethane-based membrane. Journal of Membrane Science, 2000, 170, 275-279.	8.2	19
225	Frequency-Dependent Distortion of Meridional Intensity Changes during Sinusoidal Length Oscillations of Activated Skeletal Muscle. Biophysical Journal, 2001, 80, 2809-2822.	0.5	19
226	Counterion condensation in ionic micelles as studied by a combined use of SANS and SAXS. Pramana - Journal of Physics, 2004, 63, 333-338.	1.8	19
227	In Situ Sensing of Salinity in Oriented Lipid Multilayers by Surface X-ray Scattering. Langmuir, 2004, 20, 4621-4628.	3.5	19
228	A Mesoporous Pattern Created by Nature in Spicules from Thetya aurantium Sponge. Biophysical Journal, 2007, 92, 288-292.	0.5	19
229	Deep Xâ€ray Lithography for Direct Patterning of PECVD Films. Plasma Processes and Polymers, 2010, 7, 459-465.	3.0	19
230	Reconstitution of aluminium and iron core in horse spleen apoferritin. Journal of Nanoparticle Research, 2011, 13, 6149-6155.	1.9	19
231	The 1-Monooleoyl-rac-glycerol/n-Octyl-β-d-Clucoside/Water System. Phase Diagram and Phase Structures Determined by NMR and X-ray Diffraction. Langmuir, 2003, 19, 5813-5822.	3.5	18
232	Investigation of CuInS ₂ Thin Film Formation by a Low-Temperature Chemical Deposition Method. ACS Applied Materials & Interfaces, 2012, 4, 382-390.	8.0	18
233	SAXS structural study of PrPScreveals ~11 nm diameter of basic double intertwined fibers. Prion, 2013, 7, 496-500.	1.8	18
234	Ruthenium based photosensitizer/catalyst supramolecular architectures in light driven water oxidation. Inorganica Chimica Acta, 2017, 454, 171-175.	2.4	18

#	Article	IF	CITATIONS
235	Polymorphism of human telomeric quadruplexes with drugs: a multi-technique biophysical study. Physical Chemistry Chemical Physics, 2020, 22, 11583-11592.	2.8	18
236	In situ small-angle X-ray scattering reveals solution phase discharge of Li–O ₂ batteries with weakly solvating electrolytes. Proceedings of the National Academy of Sciences of the United States of America, 2021, 118, .	7.1	18
237	Supramolecular Chalcogenâ€Bonded Semiconducting Nanoribbons at Work in Lighting Devices. Angewandte Chemie - International Edition, 2022, 61, .	13.8	18
238	Structural Diversity in Multicomponent Nanocrystal Superlattices Comprising Lead Halide Perovskite Nanocubes. ACS Nano, 2022, 16, 7210-7232.	14.6	18
239	Microstructural Parameters in Large Strain Deformed Ni Polycrystals as Investigated by Synchrotron Radiation. Physica Status Solidi A, 1999, 175, 501-511.	1.7	17
240	Structure of CdS–arachidic acid composite LB multilayers. Colloids and Surfaces A: Physicochemical and Engineering Aspects, 2002, 198-200, 59-66.	4.7	17
241	Counterion condensation on charged micelles in an aqueous electrolyte solution as studied with combined small-angle neutron scattering and small-angle x-ray scattering. Journal of Physics Condensed Matter, 2006, 18, 11399-11410.	1.8	17
242	Observation of a Rectangular DNA Superlattice in the Liquid-Crystalline Phase of Cationic Lipid/DNA Complexes. Journal of the American Chemical Society, 2007, 129, 10092-10093.	13.7	17
243	Physical and electrical properties of low dielectric constant self-assembled mesoporous silica thin films. Microelectronics Reliability, 2007, 47, 759-763.	1.7	17
244	Time-Resolved in Situ Raman and Small-Angle X-ray Diffraction Experiments: From Silica-Precursor Hydrolysis to Development of Mesoscopic Order in SBA-3 Surfactant-Templated Silica. Chemistry of Materials, 2008, 20, 1161-1172.	6.7	17
245	Hybrid Organicâ^'Inorganic Mesostructured Membranes: Interfaces and Organization at Different Length Scales. Journal of Physical Chemistry C, 2010, 114, 11730-11740.	3.1	17
246	Twist-grain boundary phase induced by Au nanoparticles in a chiral liquid crystal host. Liquid Crystals, 2017, 44, 1575-1581.	2.2	17
247	Two-Dimensional Lipid Mixing Entropy Regulates the Formation of Multicomponent Lipoplexes. Journal of Physical Chemistry B, 2006, 110, 20829-20835.	2.6	17
248	Two-dimensional perovskites with alternating cations in the interlayer space for stable light-emitting diodes. Nanophotonics, 2021, 10, 2145-2156.	6.0	17
249	Molecular packing in cadmium and zinc arachidate LB multilayers. Colloids and Surfaces A: Physicochemical and Engineering Aspects, 2002, 198-200, 75-81.	4.7	16
250	Temperature dependence of chaperone-like activity and oligomeric state of αB-crystallin. Biochimica Et Biophysica Acta - Proteins and Proteomics, 2006, 1764, 677-687.	2.3	16
251	Influence of confinement in controlled-pore glass on the layer spacing of smectic- <mml:math xmlns:mml="http://www.w3.org/1998/Math/MathML" display="inline"><mml:mi>A</mml:mi>liquid crystals. Physical Review E, 2009, 79, 051703.</mml:math 	2.1	16
252	Effect of Ceramide on Nonraft Proteins. Journal of Membrane Biology, 2009, 231, 125-132.	2.1	16

#	Article	IF	CITATIONS
253	Experimental set-up for time resolved small angle X-ray scattering studies of nanoparticles formation using a free-jet micromixer. Nuclear Instruments & Methods in Physics Research B, 2010, 268, 329-333.	1.4	16
254	SAXS Analysis of Catalyst Degradation in High Temperature PEM Fuel Cells Subjected to Accelerated Ageing Tests. Fuel Cells, 2014, 14, 938-944.	2.4	16
255	Mechanistic study of the nucleation and conformational changes of polyamines in presence of phosphate ions. Journal of Colloid and Interface Science, 2019, 543, 335-342.	9.4	16
256	Structural insights into fusion mechanisms of small extracellular vesicles with model plasma membranes. Nanoscale, 2021, 13, 5224-5233.	5.6	16
257	Synchrotron X-ray study at Trieste: No correlation between breast cancer and hair structure. Synchrotron Radiation News, 1999, 12, 32-34.	0.8	15
258	Investigation on precipitation in Zircaloy-2 fuel cladding tube. Journal of Alloys and Compounds, 2000, 308, 250-258.	5.5	15
259	Effects of the Number of Actin-Bound S1 and Axial Force on X-Ray Patterns of Intact Skeletal Muscle. Biophysical Journal, 2006, 90, 975-984.	0.5	15
260	Effect of Sodium Dodecyl Sulfate at Different Hydration Conditions on Dioleoyl Phosphatidylcholine Bilayers Studied by Grazing Incidence X-ray Diffraction. Langmuir, 2006, 22, 5256-5260.	3.5	15
261	Formation of overcharged cationic lipid/DNA complexes. Chemical Physics Letters, 2006, 429, 250-254.	2.6	15
262	Scanning x-ray microdiffraction of optically manipulated liposomes. Applied Physics Letters, 2007, 91, 234107.	3.3	15
263	A high volume and low damage route to hydroxyl functionalization of carbon nanotubes using hard X-ray lithography. Carbon, 2013, 51, 430-434.	10.3	15
264	Cantilever bending based on humidity-actuated mesoporous silica/silicon bilayers. Beilstein Journal of Nanotechnology, 2016, 7, 637-644.	2.8	15
265	Nanofibers versus Nanopores: A Comparison of the Electrochemical Performance of Hierarchically Ordered Porous Carbons. ACS Applied Energy Materials, 2019, 2, 5279-5291.	5.1	15
266	Interplay Among Dealloying, Ostwald Ripening, and Coalescence in Pt <i>_X</i> Ni _{100–<i>X</i>} Bimetallic Alloys under Fuel-Cell-Related Conditions. ACS Catalysis, 2021, 11, 11360-11370.	11.2	15
267	Membrane Phase Drives the Assembly of Gold Nanoparticles on Biomimetic Lipid Bilayers. Journal of Physical Chemistry C, 2022, 126, 4483-4494.	3.1	15
268	Nanocrystallisation of amorphous alloys: comparison between furnace and current annealing. Intermetallics, 2000, 8, 287-291.	3.9	14
269	Molecular packing in CdS containing conducting polymer composite LB multilayers. Colloids and Surfaces A: Physicochemical and Engineering Aspects, 2002, 198-200, 67-74.	4.7	14
270	Self-organization of polyaniline nanorods: Towards achieving a higher conductivity. Applied Physics Letters, 2005, 87, 093117.	3.3	14

#	Article	IF	CITATIONS
271	Guanosine Quadruplexes in Solution: A Small-Angle X-Ray Scattering Analysis of Temperature Effects on Self-Assembling of Deoxyguanosine Monophosphate. Journal of Nucleic Acids, 2010, 2010, 1-10.	1.2	14
272	Growth Mechanism of Cadmium Sulfide Nanocrystals. Journal of Physical Chemistry Letters, 2010, 1, 304-308.	4.6	14
273	Mesoporous SiO2thin films containing photoluminescent ZnO nanoparticles and simultaneous SAXS/WAXS/ellipsometry experiments. Journal of Materials Chemistry, 2011, 21, 1139-1146.	6.7	14
274	X-ray lithography and small-angle X-ray scattering: a combination of techniques merging biology and materials science. European Biophysics Journal, 2012, 41, 851-861.	2.2	14
275	Architecturing Nanospace via Thermal Rearrangement for Highly Efficient Gas Separations. Journal of Physical Chemistry C, 2013, 117, 24654-24661.	3.1	14
276	<i>SAXSDOG</i> : open software for real-time azimuthal integration of 2D scattering images. Journal of Applied Crystallography, 2022, 55, 677-685.	4.5	14
277	DNA release from cationic liposome/DNA complexes by anionic lipids. Applied Physics Letters, 2006, 89, 233903.	3.3	13
278	Polymer-Assisted Synthesis of Two-Dimensional Silver Meso-Structures. Journal of Physical Chemistry C, 2009, 113, 11198-11203.	3.1	13
279	Form factor of an <i>N</i> -layered helical tape and its application to nanotube formation of hexa- <i>peri</i> -hexabenzocoronene-based molecules. Journal of Applied Crystallography, 2010, 43, 850-857.	4.5	13
280	Microfabrication of mesoporous silica encapsulated enzymes using deep X-ray lithography. Journal of Materials Chemistry, 2012, 22, 16191.	6.7	13
281	Selfâ€Assembly of Ferromagnetic Organic–Inorganic Perovskiteâ€Like Films. Small, 2014, 10, 4912-4919.	10.0	13
282	Ionic liquid- and surfactant-controlled crystallization of WO ₃ films. Physical Chemistry Chemical Physics, 2015, 17, 18138-18145.	2.8	13
283	Design of broadband SERS substrates by the laser-induced aggregation of gold nanoparticles. Journal of Materials Chemistry C, 2016, 4, 6152-6159.	5.5	13
284	On the formation of Bi 2 S 3 -cellulose nanocomposite films from bismuth xanthates and trimethylsilyl-cellulose. Carbohydrate Polymers, 2017, 164, 294-300.	10.2	13
285	Monoacyl phosphatidylcholine inhibits the formation of lipid multilamellar structures during in vitro lipolysis of self-emulsifying drug delivery systems. European Journal of Pharmaceutical Sciences, 2017, 108, 62-70.	4.0	13
286	µDrop: a system for high-throughput small-angle X-ray scattering measurements of microlitre samples. Journal of Applied Crystallography, 2021, 54, 132-141.	4.5	13
287	Time-resolved small angle scattering: kinetic and structural data from proteins in solution. Journal of Applied Crystallography, 2000, 33, 548-551.	4.5	12
288	Pressure Effects on Columnar Lyotropics:  Anisotropic Compressibilities in Guanosine Monophosphate Four-Stranded Helices. Journal of Physical Chemistry B, 2004, 108, 1783-1789.	2.6	12

#	Article	IF	CITATIONS
289	Bidirectional tensile testing cell for in situ small angle X-ray scattering investigations of soft tissue. Nuclear Instruments & Methods in Physics Research B, 2006, 246, 262-268.	1.4	12
290	Growth of Semiconducting Nanocrystals of CdS and ZnS. Journal of Nanoscience and Nanotechnology, 2007, 7, 1726-1729.	0.9	12
291	Facile and Controlled Synthesis of Ultraâ€∓hin Low Dielectric Constant Meso/Microporous Silica Films. ChemPhysChem, 2008, 9, 1524-1527.	2.1	12
292	Thermal induced mobility of self-assembled platelets of polyethylene-block-poly(ethylene oxide) in liquid precursors of unsaturated polyester thermoset. European Polymer Journal, 2009, 45, 2505-2512.	5.4	12
293	Patterning block copolymer thin films by deep X-ray lithography. Soft Matter, 2010, 6, 3172.	2.7	12
294	Optical Tweezers for Synchrotron Radiation Probing of Trapped Biological and Soft Matter Objects in Aqueous Environments. Analytical Chemistry, 2011, 83, 4863-4870.	6.5	12
295	Investigation of Many-Body Exciton Recombination and Optical Anisotropy in Two-Dimensional Perovskites Having Different Layers with Alternating Cations in the Interlayer Space. Journal of Physical Chemistry C, 2021, 125, 7799-7807.	3.1	12
296	Picosecond pump–probe X-ray scattering at the Elettra SAXS beamline. Journal of Synchrotron Radiation, 2020, 27, 51-59.	2.4	12
297	Small-angle X-ray scattering studies of nanophase TiO2 thin films. Materials Science and Engineering B: Solid-State Materials for Advanced Technology, 1998, 54, 174-181.	3.5	11
298	Nanostructure of sol–gel derived TiO2 for thin films on glass substrates measured by small angle scattering of synchrotron light. Materials Letters, 1998, 36, 56-60.	2.6	11
299	Trapping of short-lived intermediates in phospholipid phase transitions: The Lα* phase. Faraday Discussions, 1999, 111, 31-40.	3.2	11
300	Hybrid 3D Ordered Mesoporous Thin Films Made from Organosiloxane Precursors. Journal of Sol-Gel Science and Technology, 2003, 26, 587-591.	2.4	11
301	Development of a two-dimensional virtual-pixel X-ray imaging detector for time-resolved structure research. Journal of Synchrotron Radiation, 2004, 11, 177-186.	2.4	11
302	Time-resolved SAXS studies of periodic mesoporous organosilicas in anodic alumina membranes. Microporous and Mesoporous Materials, 2010, 130, 203-207.	4.4	11
303	Using Sol–Gel Replications to Assess the Porosity of Block-Copolymer Derived Thin Films. Journal of Physical Chemistry C, 2012, 116, 5295-5302.	3.1	11
304	Peptides at the Interface: Self-Assembly of Amphiphilic Designer Peptides and Their Membrane Interaction Propensity. Biomacromolecules, 2016, 17, 3591-3601.	5.4	11
305	Resveratrol Interaction with Lipid Bilayers: A Synchrotron X-ray Scattering Study. Langmuir, 2016, 32, 12914-12922.	3.5	11
306	New insights into the GINS complex explain the controversy between existing structural models. Scientific Reports, 2017, 7, 40188.	3.3	11

#	Article	IF	CITATIONS
307	Pressure effects on α-synuclein amyloid fibrils: An experimental investigation on their dissociation and reversible nature. Archives of Biochemistry and Biophysics, 2017, 627, 46-55.	3.0	11
308	Structural and optical properties of a perylene bisimide in aqueous media. Chemical Physics Letters, 2017, 683, 454-458.	2.6	11
309	Detection of Pancreatic Ductal Adenocarcinoma by Ex Vivo Magnetic Levitation of Plasma Protein-Coated Nanoparticles. Cancers, 2021, 13, 5155.	3.7	11
310	Formation mechanism of mesoporous silica formed with triblock copolymers; effect of salt addition. Studies in Surface Science and Catalysis, 2005, 158, 97-104.	1.5	10
311	Thin and continuous films with controlled bi- and tri-modal porosities by embedment of zeolite nanoparticles in a mesoporous matrix. Journal of Materials Chemistry, 2008, 18, 2213.	6.7	10
312	Control of silver–polymer aggregation mechanism by primary particle spatial correlations in dynamic fractal-like geometry. Nanoscale, 2011, 3, 3774.	5.6	10
313	Influence of the nanoprecipitation conditions on the supramolecular structure of squalenoyled nanoparticles. European Journal of Pharmaceutics and Biopharmaceutics, 2015, 96, 89-95.	4.3	10
314	A water-soluble, bay-functionalized perylenediimide derivative – correlating aggregation and excited state dynamics. Nanoscale, 2018, 10, 2317-2326.	5.6	10
315	Dummy-atom modelling of stacked and helical nanostructures from solution scattering data. IUCrJ, 2018, 5, 390-401.	2.2	10
316	Formation of highly ordered liquid crystalline coatings – an <i>in situ</i> GISAXS study. Physical Chemistry Chemical Physics, 2018, 20, 21903-21909.	2.8	10
317	A mechanistic explanation of the inhibitory role of the protein corona on liposomal gene expression. Biochimica Et Biophysica Acta - Biomembranes, 2020, 1862, 183159.	2.6	10
318	In situ electrochemical grazing incidence small angle X-ray scattering: From the design of an electrochemical cell to an exemplary study of fuel cell catalyst degradation. Journal of Power Sources, 2020, 477, 229030.	7.8	10
319	Peering into the Formation of Cerium Oxide Colloidal Particles in Solution by In Situ Small-Angle X-ray Scattering. Langmuir, 2020, 36, 9175-9190.	3.5	10
320	Gelling without Structuring: A SAXS Study of the Interactions among DNA Nanostars. Langmuir, 2020, 36, 10387-10396.	3.5	10
321	Bioinspired Antimicrobial Coatings from Peptide-Functionalized Liquid Crystalline Nanostructures. ACS Applied Bio Materials, 2021, 4, 5295-5303.	4.6	10
322	Human Antimicrobial Peptide Triggered Colloidal Transformations in Bacteria Membrane Lipopolysaccharides. Small, 2022, 18, e2104211.	10.0	10
323	Metal Sulfide Thin Films with Tunable Nanoporosity for Photocatalytic Applications. ACS Applied Nano Materials, 2022, 5, 1508-1520.	5.0	10
324	An Integrated Bulk and Surface Modification Strategy for Gasâ€Quenched Inverted Perovskite Solar Cells with Efficiencies Exceeding 22%. Solar Rrl, 2022, 6, .	5.8	10

#	ARTICLE	IF	CITATIONS
325	The H2-phase of the lyotropic liquid crystal sodium 3,4,5-tris(omega-acryloyloxyundecyloxy)benzoate. Liquid Crystals, 2000, 27, 407-411.	2.2	9
326	TIME-RESOLVED SAXS/WAXS STUDY OF PHASE BEHAVIOR AND CRYSTALLIZATION IN POLYMER BLENDS. Journal of Macromolecular Science - Physics, 2002, 41, 1023-1032.	1.0	9
327	A combined small-angle neutron and X-ray scattering study of block copolymers micellisation in supercritical carbon dioxide. Journal of Applied Crystallography, 2003, 36, 660-663.	4.5	9
328	Nanoimprinted Comb Structures in a Low Bandgap Polymer: Thermal Processing and Their Application in Hybrid Solar Cells. ACS Applied Materials & 2014; 10, 2014; 20	8.0	9
329	Combination of SAXS and Protein Painting Discloses the Three-Dimensional Organization of the Bacterial Cysteine Synthase Complex, a Potential Target for Enhancers of Antibiotic Action. International Journal of Molecular Sciences, 2019, 20, 5219.	4.1	9
330	Novel Core–Shell Polyamine Phosphate Nanoparticles Selfâ€Assembled from PEGylated Poly(allylamine) Tj ETQ	99918.8 rgl	3T (Overlock
331	Humidity Response of Cellulose Thin Films. Biomacromolecules, 2022, 23, 1148-1157.	5.4	9
332	SAXS measurements of azobenzene lipid vesicles reveal buffer-dependent photoswitching and quantitative <i>Z→E</i> isomerisation by X-rays. Nanophotonics, 2022, 11, 2361-2368.	6.0	9
333	Ultra small-angle scattering of neutrons from vanadium—hydrogen systems. Physica Status Solidi A, 1992, 130, 365-372.	1.7	8
334	Fast PC-based data acquisition system for gas-filled position sensitive detectors. Nuclear Instruments and Methods in Physics Research, Section A: Accelerators, Spectrometers, Detectors and Associated Equipment, 1997, 392, 384-391.	1.6	8
335	Characterization of the Nanostructures in Liquid Crystalline Mesophases Present in the Ternary System Brij-35/Dibutyl Ether/H2O by Small- and Wide-Angle X-ray Scattering. Journal of Physical Chemistry B, 1998, 102, 9161-9167.	2.6	8
336	Industrial applications of the aggregation of block copolymers in supercritical CO 2 : a SANS study. Applied Physics A: Materials Science and Processing, 2002, 74, s1427-s1429.	2.3	8
337	On the correlation between phase evolution of lipoplexes/anionic lipid mixtures and DNA release. Applied Physics Letters, 2007, 91, 143903.	3.3	8
338	Local environment of isolated iron in mesoporous silicate catalyst FeTUD-1. Microporous and Mesoporous Materials, 2007, 104, 289-295.	4.4	8
339	Time-resolved combined SAXS and WAXS studies on hydrating tricalcium silicate and cement. Advances in Cement Research, 2009, 21, 101-111.	1.6	8
340	Design of molecule-based magnetic conductors. Nano Research, 2014, 7, 1832-1842.	10.4	8
341	Getting order in mesostructured thin films, from pore organization to crystalline walls, the case of 3-glycidoxypropyltrimethoxysilane. Physical Chemistry Chemical Physics, 2015, 17, 10679-10686.	2.8	8
342	Stability and disassembly properties of human naÃ⁻ve Hsp60 and bacterial GroEL chaperonins. Biophysical Chemistry, 2016, 208, 68-75.	2.8	8

#	Article	IF	CITATIONS
343	Inter-Backbone Charge Transfer as Prerequisite for Long-Range Conductivity in Perylene Bisimide Hydrogels. ACS Nano, 2018, 12, 5800-5806.	14.6	8
344	Ligand-free preparation of polymer/CuInS ₂ nanocrystal films and the influence of 1,3-benzenedithiol on their photovoltaic performance and charge recombination properties. Journal of Materials Chemistry C, 2019, 7, 943-952.	5.5	8
345	Magnetic Levitation of Personalized Nanoparticle–Protein Corona as an Effective Tool for Cancer Detection. Nanomaterials, 2022, 12, 1397.	4.1	8
346	Smectic ordering of octylcyanobiphenyl confined to control porous glasses. Journal of Physics Condensed Matter, 2000, 12, A431-A436.	1.8	7
347	Kinetics of block-copolymer aggregation in super critical CO2. Journal of Non-Crystalline Solids, 2002, 307-310, 725-730.	3.1	7
348	Novel <i>in situ</i> setup to study the formation of nanoparticles in the gas phase by small angle x-ray scattering. Review of Scientific Instruments, 2008, 79, 043905.	1.3	7
349	Self-Organization of Synthetic Cholesteryl Oligoethyleneglycol Glycosides in Water. Langmuir, 2009, 25, 9424-9431.	3.5	7
350	Pore shape and sorption behaviour in mesoporous ordered silica films. Journal of Applied Crystallography, 2016, 49, 1713-1720.	4.5	7
351	A Shapeâ€Induced Orientation Phase within 3D Nanocrystal Solids. Advanced Materials, 2018, 30, e1802078.	21.0	7
352	Comparison of fluorene, silafluorene and carbazole as linkers in perylene monoimide based non-fullerene acceptors. Materials Advances, 2020, 1, 2095-2106.	5.4	7
353	Structural and Mechanical Properties of Silica Mesoporous Films Synthesized Using Deep X-Rays: Implications in the Construction of Devices. Frontiers in Materials, 2021, 8, .	2.4	7
354	Highly Tunable Nanostructures in a Doubly pHâ€Responsive Pentablock Terpolymer in Solution and in Thin Films. Advanced Functional Materials, 2021, 31, 2102905.	14.9	7
355	Gas gain operations with single photon resolution using an integrating ionization chamber in small-angle X-ray scattering experiments. Nuclear Instruments and Methods in Physics Research, Section A: Accelerators, Spectrometers, Detectors and Associated Equipment, 2000, 440, 181-190.	1.6	6
356	Synthesis and conformational properties of cyanoethyl–Scleroglucan. Carbohydrate Polymers, 2002, 47, 387-391.	10.2	6
357	Structural evolution of the amorphous grain boundary phase during nanocrystallisation of Fe72Cu1Nb4.5Si13.5B9. Journal of Magnetism and Magnetic Materials, 2004, 272-276, 1441-1442.	2.3	6
358	In situ studies of order–disorder phenomena in the synthesis of mesoporous silica. Journal of Non-Crystalline Solids, 2007, 353, 4823-4829.	3.1	6
359	Effect of pH on the structure of lipoplexes. Journal of Applied Physics, 2008, 104, 014701.	2.5	6
360	Mesostructured self-assembled silica films with reversible thermo-photochromic properties. Microporous and Mesoporous Materials, 2009, 120, 375-380.	4.4	6

#	Article	IF	CITATIONS
361	Local x-ray structure analysis of optically manipulated biological micro-objects. Applied Physics Letters, 2010, 97, .	3.3	6
362	Aerosol Flow Reactor with Controlled Temperature Gradient for <i>In Situ</i> Gas-Phase X-Ray Experiments—Measurements of Evaporation-Induced Self-Assembly (EISA) in Aerosols. Aerosol Science and Technology, 2011, 45, 805-810.	3.1	6
363	Organized Silica Films Generated by Evaporation-Induced Self-Assembly as Hosts for Iron Oxide Nanoparticles. Materials, 2013, 6, 1467-1484.	2.9	6
364	Real time X-ray scattering study of the formation of ZnS nanoparticles using synchrotron radiation. Materials Chemistry and Physics, 2014, 144, 310-317.	4.0	6
365	Detailed Study of the Nanocasting Process by in Situ X-ray Scattering and Diffraction. Journal of Physical Chemistry C, 2016, 120, 1854-1862.	3.1	6
366	Investigation on different chemical stability of mitochondrial Hsp60 and its precursor. Biophysical Chemistry, 2017, 229, 31-38.	2.8	6
367	Functionalized Mesoporous Thin Films for Biotechnology. Micromachines, 2021, 12, 740.	2.9	6
368	Time-resolved in-situ X-ray diffraction study of the formation of 3D-hexagonal mesoporous silica films. Materials Research Society Symposia Proceedings, 2000, 628, 1.	0.1	6
369	Honeycomb-structured copper indium sulfide thin films obtained <i>via</i> a nanosphere colloidal lithography method. Materials Advances, 2022, 3, 2884-2895.	5.4	6
370	<i>In Situ</i> Study of Nanoporosity Evolution during Dealloying AgAu and CoPd by Grazing-Incidence Small-Angle X-ray Scattering. Journal of Physical Chemistry C, 2022, 126, 4037-4047.	3.1	6
371	Low-Dimensionality Effects in the Melting of a Langmuirâ^'Blodgett Multilayer. Langmuir, 2008, 24, 7793-7796.	3.5	5
372	Nucleation and growth of CdS nanoparticles observed by ultrafast SAXS. Materials Research Society Symposia Proceedings, 2013, 1528, 1.	0.1	5
373	Role of cholesterol on the transfection barriers of cationic lipid/DNA complexes. Applied Physics Letters, 2014, 105, .	3.3	5
374	Multi-technique analysis of extracellular vesicles: not only size matters. Advances in Biomembranes and Lipid Self-Assembly, 2020, 32, 157-177.	0.6	5
375	Spatially and time-resolved SAXS for monitoring dynamic structural transitions during in situ generation of non-lamellar liquid crystalline phases in biologically relevant media. Journal of Colloid and Interface Science, 2021, 602, 415-425.	9.4	5
376	Phenyleneâ€Bridged Perylene Monoimides as Acceptors for Organic Solar Cells: A Study on the Structure–Property Relationship. Chemistry - A European Journal, 2022, 28, .	3.3	5
377	GISAXS study of defects in He implanted silicon. Materials Science and Engineering B: Solid-State Materials for Advanced Technology, 2000, 71, 82-86.	3.5	4
378	In situ formation of solid-supported lipid/DNA complexes. Chemical Physics Letters, 2005, 405, 252-257.	2.6	4

#	Article	IF	CITATIONS
379	Smectic Ordering of 8CB Liquid Crystal Confined to a Controlled-Pore Glass. Molecular Crystals and Liquid Crystals, 2005, 439, 33/[1899]-42/[1908].	0.9	4
380	Effect of annealing current density on the microstructure of nanocrystalline FeCuNbSiB alloy. Journal of Applied Physics, 2007, 101, 053907.	2.5	4
381	Mesostructured Silica Aerosol Particles: Comparison of Gas-Phase and Powder Deposit X-ray Diffraction Data. Langmuir, 2011, 27, 5542-5548.	3.5	4
382	Small-angle X-ray scattering (SAXS) study of porous anodic alumina—A new approach. Materials Chemistry and Physics, 2011, 131, 362-369.	4.0	4
383	Synchrotron Small-Angle X-ray Scattering Studies of Hemoglobin Nonaggregation Confined inside Polymer Capsules. Journal of Physical Chemistry B, 2012, 116, 9604-9610.	2.6	4
384	Thorough small-angle X-ray scattering analysis of the instability of liquid micro-jets in air. Journal of Synchrotron Radiation, 2014, 21, 193-202.	2.4	4
385	Laser ablation and injection moulding as techniques for producing micro channels compatible with Small Angle X-Ray Scattering. Microelectronic Engineering, 2018, 195, 7-12.	2.4	4
386	Gene Therapy: Encapsulation, Visualization and Expression of Genes with Biomimetically Mineralized Zeolitic Imidazolate Frameworkâ€8 (ZIFâ€8) (Small 36/2019). Small, 2019, 15, 1970193.	10.0	4
387	The effect of CoPt-coated reduced-graphene oxide nanosheets upon the Smectic-A to Smectic-C* phase transition of a chiral liquid crystal. Liquid Crystals, 2020, 47, 831-837.	2.2	4
388	The boundary lipid around DMPC-spanning influenza A M2 transmembrane domain channels: Its structure and potential for drug accommodation. Biochimica Et Biophysica Acta - Biomembranes, 2020, 1862, 183156.	2.6	4
389	Metal–Insulator Transition of Ultrathin Sputtered Metals on Phenolic Resin Thin Films: Growth Morphology and Relations to Surface Free Energy and Reactivity. Nanomaterials, 2021, 11, 589.	4.1	4
390	Studies on the 14.5 nm Meridional X-Ray Diffraction Reflection During Length Changes of Intact Frog Muscle Fibres. Advances in Experimental Medicine and Biology, 1998, 453, 247-258.	1.6	4
391	The potential of asymmetric monochromator crystals for use in highâ€power insertionâ€device Beamlines. Synchrotron Radiation News, 1995, 8, 22-27.	0.8	3
392	X-ray scattering measurements on nanosized TiO2 micelles. Solar Energy Materials and Solar Cells, 1999, 59, 387-392.	6.2	3
393	Orientational ordering in polymorphic terepthal-bis-4-butylaniline (TBBA). Solid State Communications, 2002, 122, 329-333.	1.9	3
394	Myosin lever disposition during length oscillations when power stroke tilting is reduced. American Journal of Physiology - Cell Physiology, 2005, 289, C177-C186.	4.6	3
395	Fracture of poly(vinylidene fluoride): a combined synchrotron and laboratory in-situ X-ray scattering study. Journal of Applied Crystallography, 2007, 40, s564-s567.	4.5	3
396	Simultaneous in situ and Time-Resolved Study of Hierarchical Porous Films Templated by Salt Nanocrystals and Self-Assembled Micelles. Journal of Physical Chemistry C, 2011, 115, 12702-12707.	3.1	3

#	Article	IF	CITATIONS
397	Segregation into domains observed in liquid crystal phases: comparison of experimental and theoretical data. Soft Matter, 2011, 7, 3392.	2.7	3
398	Dynamic templating role of polynaphtalene sulphonate in the formation of silver nanocrystals in aqueous solution. Journal of Nanoparticle Research, 2011, 13, 3107-3112.	1.9	3
399	Time-resolved structure investigation with small angle X-ray scattering using scanning techniques. Rendiconti Lincei, 2011, 22, 93-107.	2.2	3
400	Effects of the regulatory ligands calcium and GTP on the thermal stability of tissue transglutaminase. Amino Acids, 2012, 42, 2233-2242.	2.7	3
401	Probing hemoglobin confinement inside submicron silica tubes using synchrotron SAXS and electrochemical response. European Biophysics Journal, 2013, 42, 371-382.	2.2	3
402	Structural characterization of cationic liposome/poly(I:C) complexes showing high ability in eliminating prostate cancer cells. RSC Advances, 2013, 3, 24597.	3.6	3
403	Structural Study of the Hydration of Lipid Membranes Upon Interaction With Mesoporous Supports Prepared by Standard Methods and/or Xâ€Ray Irradiation. Frontiers in Materials, 2021, 8, .	2.4	3
404	SAXS Reveals the Stabilization Effects of Modified Sugars on Model Proteins. Life, 2022, 12, 123.	2.4	3
405	Patterning a cellulose based dual-tone photoresist via deep X-ray lithography. Microelectronic Engineering, 2022, 256, 111720.	2.4	3
406	Supramolecular Chalcogenâ€Bonded Semiconducting Nanoribbons at Work in Lighting Devices. Angewandte Chemie, 2022, 134, .	2.0	3
407	Novel detector systems for time resolved SAXS experiments. Journal of Applied Crystallography, 2000, 33, 778-781.	4.5	2
408	Timeâ€resolved small angle scattering in soft condensed matter and biological systems. Synchrotron Radiation News, 2002, 15, 27-31.	0.8	2
409	Phase transformations involved during silica, modified silica, and non-silica mesoporous-organized thin films deposition. The role of evaporation Studies in Surface Science and Catalysis, 2003, 146, 281-284.	1.5	2
410	Elucidation of the isomeric domains formed by sodium N-dodecanoyl-l-prolinate. Journal of Colloid and Interface Science, 2004, 280, 212-218.	9.4	2
411	On the mechanism of formation of SBA-1 and SBA-3 as studied by in situ synchrotron XRD. Studies in Surface Science and Catalysis, 2008, , 103-108.	1.5	2
412	The role of etched silicon channels on the pore ordering of mesoporous silica: The importance of film thickness on providing highly orientated and defect-free thin films. Applied Surface Science, 2009, 255, 9333-9342.	6.1	2
413	Disorder-Order-Crystalline State Transitions of PEO- <i>b</i> -PPO- <i>b</i> -PEO Copolymers and their Blends: SAXS/WAXS/DSC Study. Journal of Macromolecular Science - Physics, 2009, 48, 174-184.	1.0	2
414	Phase diagram of 3β-[N-(N,N-dimethylaminoethane)-carbamoyl]- cholesterolâ°'dioleoylphosphatidylethanolamine/DNA complexes suggests strategies for efficient lipoplex transfection. Applied Physics Letters, 2010, 96, 183703.	3.3	2

#	Article	IF	CITATIONS
415	High Hydrostatic Pressure Induces a Lipid Phase Transition and Molecular Rearrangements in Lowâ€Density Lipoprotein Nanoparticles. Particle and Particle Systems Characterization, 2018, 35, 1800149.	2.3	2
416	A DNA origami plasmonic sensor with environment-independent read-out. Nano Research, 2019, 12, 2900-2907.	10.4	2
417	Antituberculosis Drug Interactions with Membranes: A Biophysical Approach Applied to Bedaquiline. Membranes, 2019, 9, 141.	3.0	2
418	Templateâ€Mediated Control over Polymorphism in the Vaporâ€Assisted Formation of Zeolitic Imidazolate Framework Powders and Films. Angewandte Chemie, 2021, 133, 7631-7636.	2.0	2
419	Use of Sinusoidal Length Oscillations to Detect Myosin Conformation by Time- Resolved X-Ray Diffraction. Advances in Experimental Medicine and Biology, 2003, 538, 267-277.	1.6	2
420	Experimental Analysis on the Influence of Operating Profiles on High Temperature Polymer Electrolyte Membrane Fuel Cells. Energies, 2021, 14, 6737.	3.1	2
421	Blockâ€Copolymers Enable Direct Reduction and Structuration of Noble Metalâ€Based Films. Small, 2022, 18, e2104204.	10.0	2
422	Unravelling the origin of the capacitance in nanostructured nitrogen-doped carbon - NiO hybrid electrodes deposited with laser. Ceramics International, 2022, 48, 15877-15888.	4.8	2
423	<title>Time-resolved SAXS/WAXS study of polymer blend crystallization</title> ., 2000, , .		1
424	Morphology of solid polymer electrolytes: a TR WAXS investigation. Physica A: Statistical Mechanics and Its Applications, 2002, 304, 129-134.	2.6	1
425	In-situ studies of the formation mechanism of SBA-15. Studies in Surface Science and Catalysis, 2005, 156, 69-74.	1.5	1
426	Combined laser trapping and small-angle x-ray scattering experiment for the study of liposome colloidal microparticles. , 2006, , .		1
427	Fragmentation in Large Strain Cold Rolled Aluminium as Observed by Synchrotron X-Ray Bragg Peak Profile Analysis (SXPA), Electron Back Scatter Patterning (EBSP) and Transmission Electron Microscopy (TEM). , 2000, , 163-171.		1
428	Investigation on a MMACHC mutant from cblC disease: The c.394C>T variant. Biochimica Et Biophysica Acta - Proteins and Proteomics, 2022, 1870, 140793.	2.3	1
429	Contributory presentations/posters. Journal of Biosciences, 1999, 24, 33-198.	1.1	0
430	Preliminary results of a combined USAXS and diffraction enhanced imaging system with synchrotron radiation. , 0, , .		0
431	In situ SAXS/XRD on mesoscopically ordered surfactant-silica mesophases; What can we learn?. Materials Research Society Symposia Proceedings, 2004, 847, 374.	0.1	0
432	In situ high pressure phase transition of alcohol intercalated zirconium phosphate observed by synchrotron X-ray scattering. Journal of Physics and Chemistry of Solids, 2004, 65, 615-618.	4.0	0

#	Article	IF	CITATIONS
433	Thermally Stable Nanocrystalline γ-Alumina Layers with Highly Ordered 3D Mesoporosity ChemInform, 2005, 36, no.	0.0	0
434	Phospholipid Mesophases at Solid Interfaces: In situ X-Ray Diffraction and Spin-Label Studies. ChemInform, 2005, 36, no.	0.0	0
435	Optical Tweezers for Sample Fixing in Micro-Diffraction Experiments. AIP Conference Proceedings, 2007, , .	0.4	0
436	In-situ X-ray diffraction study on the formation of a periodic mesoporous organosilica material. Studies in Surface Science and Catalysis, 2007, 165, 9-12.	1.5	0
437	Multifunctional Integrated Platforms: Fabrication of Advanced Functional Devices Combining Soft Chemistry with Xâ€ray Lithography in One Step (Adv. Mater. 48/2009). Advanced Materials, 2009, 21, .	21.0	0
438	Scattering techniques in biology—Marking the contributions to the field from Peter Laggner on the occasion of his 68th birthday. European Biophysics Journal, 2012, 41, 777-779.	2.2	0
439	Nanocrystals: A Shape-Induced Orientation Phase within 3D Nanocrystal Solids (Adv. Mater. 32/2018). Advanced Materials, 2018, 30, 1870235.	21.0	0
440	Correction: Structural insights into fusion mechanisms of small extracellular vesicles with model plasma membranes. Nanoscale, 2021, 13, 13158-13158.	5.6	0
441	Perovskite-type nanocrystal superlattices from lead halide perovskite nanocubes. , 0, , .		0
442	Novel Core–Shell Polyamine Phosphate Nanoparticles Selfâ€Assembled from PEGylated Poly(allylamine) Tj ETQ 17, 2170182.	90000rgl 10.0	BT /Overlock 0
443	Deep X-ray lithography on "sol–gel―processed noble metal mesoarchitectured films. Nanoscale, 2022, 14, 1706-1712.	5.6	0
444	Structural Diversity in Multicomponent Nanocrystal Superlattices Comprising Lead Halide Perovskite Nanocubes. , 0, , .		0
445	Selfâ€Assembly of Oriented Antibodyâ€Decorated Metal–Organic Framework Nanocrystals for Activeâ€Targeting Applications (Adv. Mater. 21/2022). Advanced Materials, 2022, 34, .	21.0	0